# Conditions of Strongest Electromagnetic Power Deposition in Man and Animals

O. P. GANDHI, SENIOR MEMBER, IEEE

*Abstract*—**Strongest power deposition for biological bodies is found for fields polarized along the longest dimension for frequencies such that the major length is about 0.4 times the free-space wavelength of radiation. Peak absorption in the presence of ground effects is observed at frequencies about one-half as much as for bodies isolated in free space. At resonance, an effective absorption area 3–4 times the shadow cross section is measured. Using biological-phantom figurines of the human body, distribution of power absorption is determined. Maximum power deposition is observed for the neck region. Initial experiments with anesthetized and dead rats have confirmed this observation.**

## INTRODUCTION

BECAUSE of the expanding uses of electromagnetic (EM) radiation, it has become necessary to establish the most hazardous conditions of exposure to such radiation for humans. In particular, it is important to know the frequency regions of most absorption for various orientations of the body relative to the polarization of incident waves and how the absorption cross section varies with frequency of EM radiation. It is also important to determine the distribution of power absorption in the body to ascertain locations of maximum deposition particularly close to resonant frequencies. This knowledge is vital in evaluating and establishing radiation safety standards.

Based on our previous experiments [1] with rats and biological-phantom and saline-filled prolate spheroidal bodies, strongest whole-body absorption was found for EM fields polarized with electric field along the long dimensions of the bodies. EM power absorption was measured for bodies of fixed size at various frequencies using a parallel-plate waveguide as a transmission medium of plane waves and compared [2] with data obtained from fixed-frequency free-space irradiation exposures of bodies of varying sizes. The salient features of the experimentally observed results (qualitatively sketched in Fig. 1) are as follows.

1) The $\boldsymbol{E} \parallel \hat{L}$ orientation is found to be the most absorbing, and $\boldsymbol{H} \parallel \hat{L}$ the least absorbing, with the configuration $\boldsymbol{k} \parallel \hat{L}$ only slightly more absorbing than the $\boldsymbol{H} \parallel \hat{L}$ orientation. The vectors $\boldsymbol{E}$, $\boldsymbol{H}$, and $\boldsymbol{k}$ are along the electric and magnetic fields, and along the direction of propagation, respectively, and $\hat{L}$ is along the major length $L$ of the body. These experimental results are in qualitative agreement with recent theoretical results [3] on power absorption in homogeneous lossy prolate spheroids. Quantitative comparison has not been possible because of the long-wavelength ($kL \lesssim 0.6$) approximation of the theory. By contrast, the experimental results pertain mostly to frequencies on the order of resonant and higher frequencies ($kL \gtrsim 1.0$).

2) The frequencies of peak absorption occur in the reverse order. Maximum absorption for $\boldsymbol{E} \parallel \hat{L}$ occurs at the lowest frequency with $kL = 2\pi L/\lambda$ on the order of

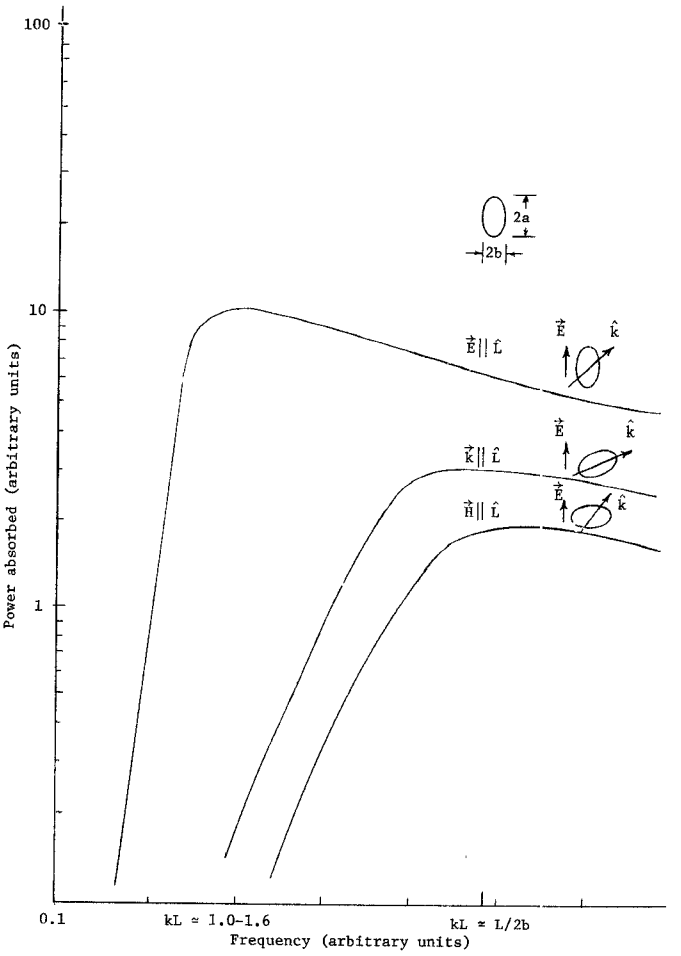


Fig. 1. Typical RF absorption curves for animals and bodies of prolate-spheroidal shape obtained with a parallel-plate waveguide. Symbols with arrows above are represented by boldface italic in text.

Manuscript received April 15, 1975; revised August 26, 1975. This work was supported by the U. S. Army Medical Research and Development Command under Contract DAMD 17-74-C-4092.

The author is with the Department of Electrical Engineering, University of Utah, Salt Lake City, Utah 84112. He is also a consultant to the Division of Neuropsychiatry, Walter Reed Army Institute of Research, Washington, D. C. 20012.

TABLE I
ACTUAL AND EQUIVALENT PROLATE SPHEROIDAL DIMENSIONS FOR ANESTHETIZED RATS OF DIFFERENT WEIGHTS

| Weight of the Rat in Grams | Rat Length l from Nose to Base of Tail cm | Measured Circumference of the Animal cms | Nominal Circumference* $2\pi b$ in cms | Aspect Ratio $L/2b$ of Equivalent Prolate Spheroid |
|---|---|---|---|---|
| 96 | 15.5 | 11.5 (body) max. 9.0 (head) | 10.80 | 4.50 |
| 158 | 18.0 | 13.5 (body) max. 9.0 (head) | 12.82 | 4.30 |
| 261 | 21.0 | 15.0 (body) max. 10.0 (head) | 15.32 | 4.30 |
| 390 | 23.5 | 18.0 (body) max. 11.0 (head) | 17.70 | 4.35 |

* This is calculated from the relationship $2/3\ \pi L b^2 \bar{\rho} = W$.

1.0 to 1.6 ($L/\lambda \simeq 0.16$ to 0.25). Peak absorption for $\boldsymbol{k} \parallel \hat{L}$ and $\boldsymbol{H} \parallel \hat{L}$ orientations occurs at successively higher frequencies, with $kL$ for these configurations on the order of $L/2b$ where $2b$ is the length of the equivalent prolate spheroidal body[1] along the minor axes (see Table I for numbers illustrative of 90–400-g rats). These values of $kL$ for resonance in the different orientations are obtained approximately by requiring that for a sphere [4], [5] the shortest circumference for the lossy creeping waves launched at the center of the shadow plane be 0.5 λ.

3) In the frequency region immediately below resonance, absorption diminishes rapidly with frequency. An $f^{4.75}$ dependence similar to that for spheres is observed.

4) There is an excellent correlation of the results obtained from the parallel-plate waveguide with the free-space irradiation results [1], [2]. The only exception is that maximum absorption in the free-space case occurs for body size of about 0.4 λ, i.e., at approximately twice the frequency observed in the parallel-plate waveguide situation. The reason for this may be that while a body isolated in free space is required to be approximately 0.4 λ for resonance, the same condition is met in the presence of a ground plane (such as in the parallel-plate waveguide) with only a 0.2-λ body and its image in the ground plane acting together.

## CORRELATION WITH LETHALITY RESULTS

A study [6] has just been completed at Walter Reed Army Institute of Research, Washington, D. C., on the lethality of 100–125- and 380–420-g rats and 25–35-g mice when exposed to microwave radiation at 710, 985, 1700, 2450, and 3000 MHz. The choice of frequencies was dictated by the anechoic chamber facilities available at Walter Reed Laboratories. The time to convulsion was measured for $\boldsymbol{E} \parallel \hat{L}$ and $\boldsymbol{H} \parallel \hat{L}$ configurations. At each frequency, eleven animals were studied for each of the two orientations picked to correspond to the maximum and minimum absorbing configurations of Fig. 1. The lethality data correlate well with our results [1], [2] obtained from the modeling experiments. In particular, the following points of agreement are noteworthy.

1) The time to convulsion in the $\boldsymbol{E} \parallel \hat{L}$ orientation is always shorter than that for the $\boldsymbol{H} \parallel \hat{L}$ orientation.[2]

2) On the low-frequency side of resonance, the time to convulsion rises very rapidly, corresponding to a fast diminishing absorption in this region (see Fig. 1).

3) The minimum time to convulsion for $\boldsymbol{H} \parallel \hat{L}$ orientation occurs for $kL \simeq 4.4$. From Table I, the nominal $L/2b$ for rats of different weights is on the order of 4.4. The lethality results are consequently in agreement with the parallel-plate waveguide results for resonant absorption at $kL \simeq L/2b$.

4) For the $\boldsymbol{E} \parallel \hat{L}$ configuration, minimum time to convulsion is obtained at frequencies such that the length from the animal's eyes to the base of the tail is approximately 0.4 λ. This is in agreement with the free-space experiments described in the following (see Fig. 2) and also in [1].

## SCALING

To evaluate the validity of scaling, free-space heating experiments were repeated[3] at 710 MHz for saline-filled prolate spheroidal bodies ($L/2b = 6$ corresponding to humans) of major length varying from 7.6 to 25.4 cm. The temperature increase for a 5-min exposure to 100-mW/cm² radiation is plotted in Fig. 2. From the amount of energy absorbed, the relative absorption coefficient [7] $S$

[1] The dimension $2b$ for an equivalent prolate spheroid is calculated from the expression $2/3\ \pi b^2 L \bar{\rho} = W$, where $W$ is the weight of the body and $\bar{\rho}$ is the average mass density of nearly 1 g/cm³. The nominal circumference $2\pi b$ so calculated has been found to correspond well to the average circumference actually measured for rats of weights varying from 90 to 400 g (see Table I).

[2] The only exception to this observation is 400-g rats at 2450 and 3000 MHz. For these animals, such frequencies are 4–5 times higher than the resonant frequency of the $\boldsymbol{E} \parallel \hat{L}$ orientation. A considerably reduced total power deposition under these circumstances may well be the reason for this anomaly.

[3] Experiments were previously done at 1700 MHz with smaller size prolate spheroidal bodies with $L$ of 4.8, 6, 7.2, 9.6, and 14.4 cm (see [1]).

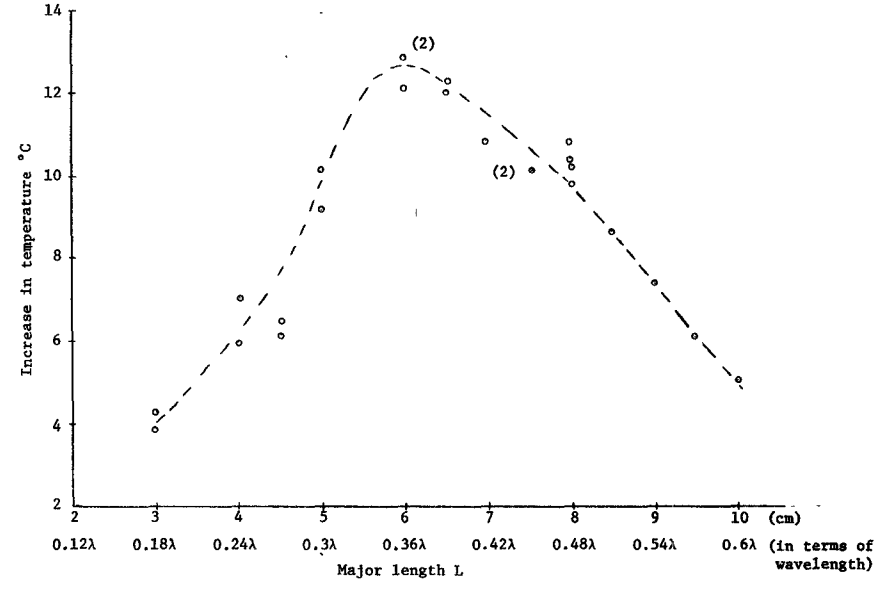


Fig. 2. Temperature rise in saline-filled prolate spheroids with an aspect ratio $L/2b$ of 6. Frequency, 710 MHz; irradiation time, 5 min; incident power density, 100 mW/cm²; polarization, $\boldsymbol{E} \parallel \hat{L}$.

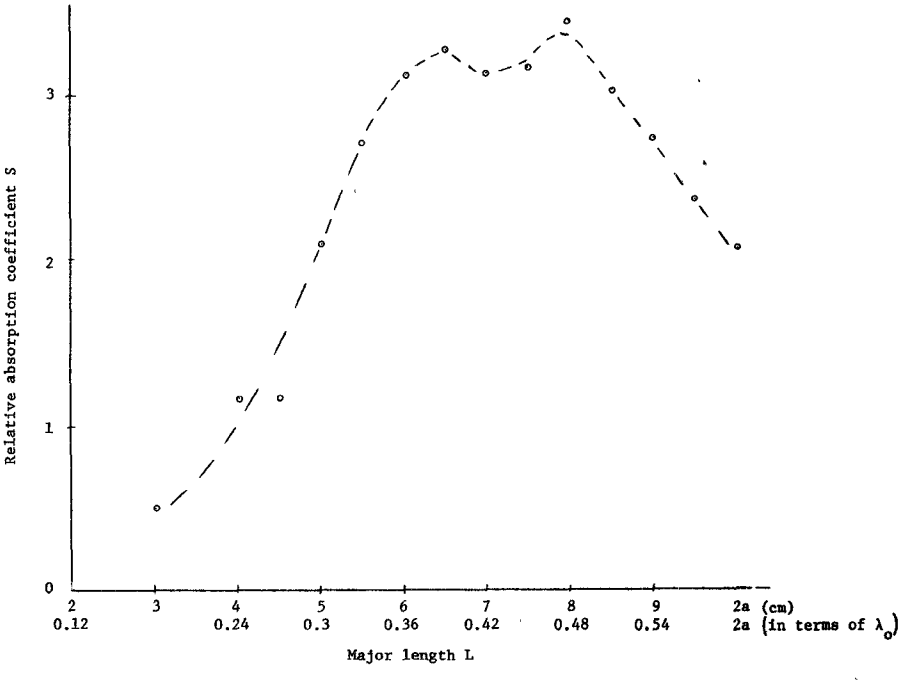


Fig. 3. Relative absorption coefficient $S$ for different size prolate spheroids ($L/2b$ = 6 in each case). Polarization: $\boldsymbol{E} \parallel \hat{L}$.

is calculated[4] and is plotted in Fig. 3. Maximum absorption is observed, as before [1], [2], for bodies of major length on the order of 0.38–0.48 λ, and whole-body deposition of about 3.5 times as much as that called for by the shadow area is measured. This verifies experimentally the concept of scaling. Bodies scaled down in all dimensions result in peak absorption frequencies scaled up by the same factor and vice versa.

## CORE TEMPERATURE OF RATS EXPOSED IN DIFFERENT ORIENTATIONS

In order to dramatize the polarization-dependent variability of the EM hazard, 250-g[5] Wistar rats were exposed to 100-mW/cm² fields. The rectal temperature of the animal was measured under irradiation, using the

[4] The relative absorption coefficient $S$ is defined as the absorption cross section divided by the physical-shadow cross section. Power absorbed in milliwatts = (4180 × temperature increase of the body × weight in grams)/irradiation time in seconds. This divided by the incident field intensity in milliwatts/square centimeter gives the absorption cross section.

[5] This particular weight was selected to observe the $L \simeq 0.4$-λ condition for maximum absorption in the free space.

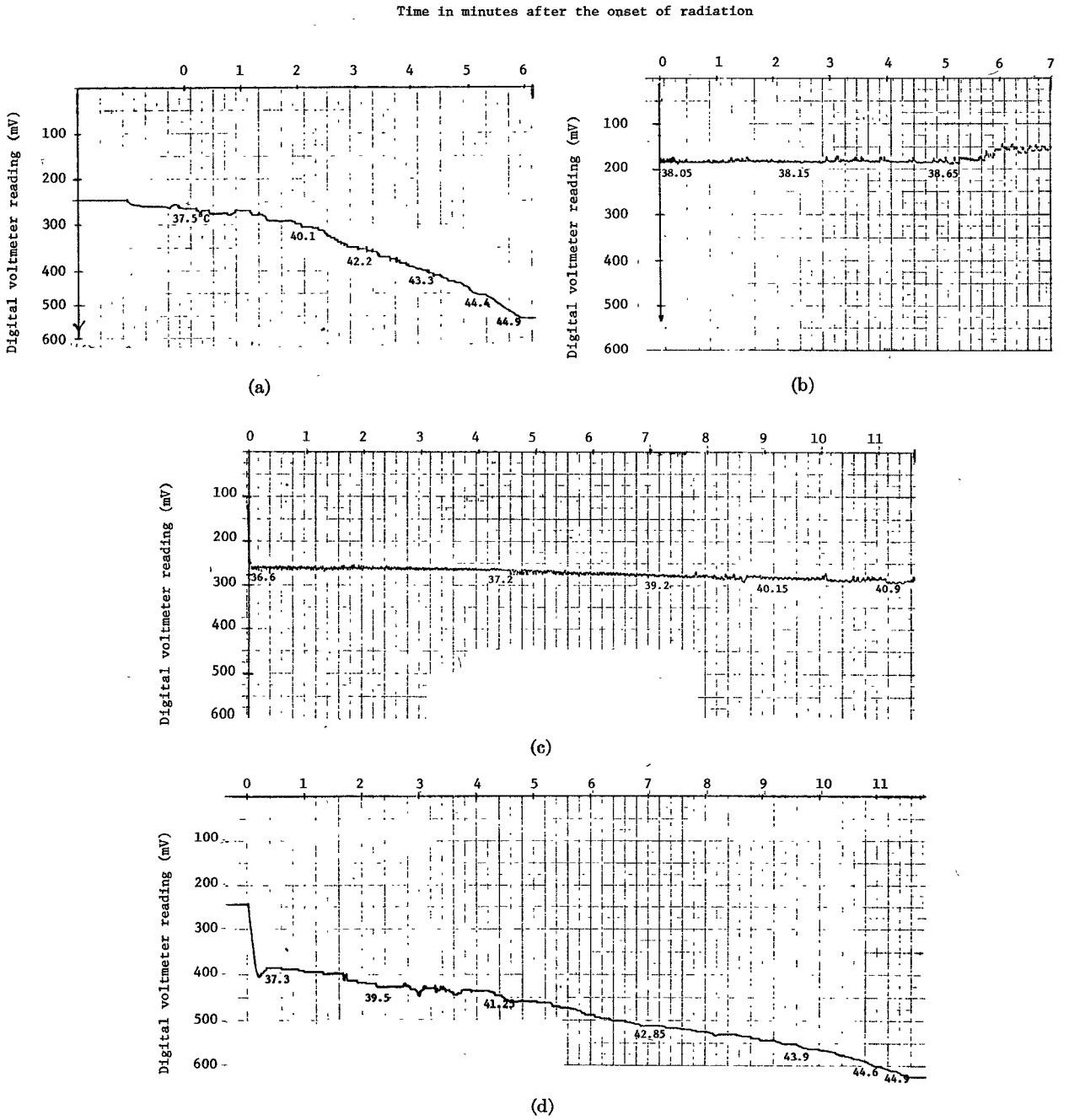


Fig. 4. Core temperature of 250-g rats exposed to 710-MHz radiation. (a) Orientation $\boldsymbol{E} \parallel \hat{L}$; incident power density, 100 mW/cm². (b) Orientation $\boldsymbol{K} \parallel \hat{L}$; incident power density, 100 mW/cm². (c) Orientation $\boldsymbol{H} \parallel \hat{L}$; incident power density, 100 mW/cm². (d) Orientation $\boldsymbol{E} \parallel \hat{L}$; incident power density, 50 mW/cm².

relatively nonperturbing liquid-crystal fiberoptic temperature probe [8]. The digital voltmeter reading as a function of time was recorded and is given in Fig. 4(a), (b), and (c) for the three orientations. The core temperature read off the calibration chart of the probe is marked alongside the curves in Fig. 4. For an incident power density of 50 mW/cm² [Fig. 4(d)], the power deposition in the $\boldsymbol{E} \parallel \hat{L}$ orientation was still much higher than that for the other two configurations at 100 mW/cm². The increase in animal temperature as a function of time for the two power densities in the $\boldsymbol{E} \parallel \hat{L}$ orientation is plotted in Fig. 5. For this configuration, the relative absorption coefficients $S$ of 3.8 and 4.26 are calculated from the initial slopes of the temperature-rise curves for 100- and 50-mW/cm² incident field intensities, respectively. This may be compared to $S$ on the order of 3.5 for resonant-size saline-filled prolate spheroids (Fig. 3).

## DISTRIBUTION OF POWER DEPOSITION—"HOT SPOTS"

To determine the distribution of power deposition, an 18.4-cm-tall figurine of the female body has been used as a mold to form a cavity in styrofoam. The size of the figurine has been selected such as to allow resonance (Fig. 3) at

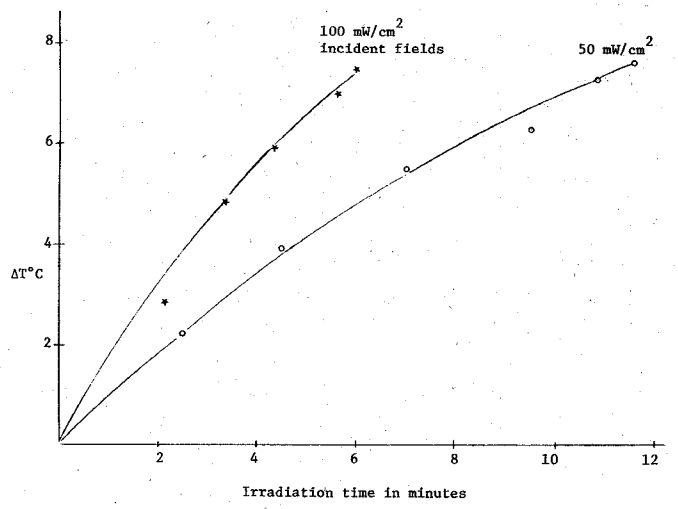


Fig. 5. Core temperature increase of 250-g Wistar rats exposed to 710-MHz free-space radiation ($\boldsymbol{E} \parallel \hat{L}$ orientation).

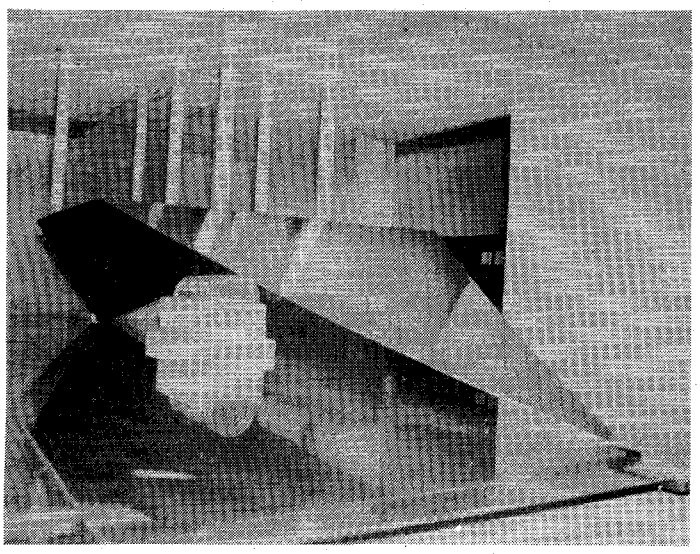

Fig. 6. Photograph of the parallel-plate radiation chamber.

710 MHz for free-space radiation ($L/\lambda \simeq 0.44$) and at a frequency about half as much in the parallel-plate radiation chamber. In order to simulate ground effects on EM power absorption, a larger parallel-plate radiation chamber (Fig. 6) has been designed and fabricated. For the chamber, the central working area[6] consists of a copper plate of 63.5-cm width separated by a 25.4-cm clearance from the ground plate of 117-cm width. The overall transmission length of 198 cm is occupied by two symmetrical tapered sections of 61-cm axial length, the central working area of 61-cm length, and the 7.5-cm end sections connected to UG58/U input and output coaxial connectors.

From EM field theory, a body reduced by a factor of $\beta$ in all dimensions may be used to obtain RF absorption characteristics of the full-scale body, provided an irradiation frequency scaled up by a factor of $\beta$ is used. However, it is necessary that the complex permittivity $(\epsilon_1 - j\sigma/\omega\epsilon_0)$ represented by the scaled-down model correspond to the value at the lower frequency characteristic of the whole body. With these scaling precautions, the distribution of power deposition in the reduced scale model is identical (though the magnitudes are higher by a factor of $\beta$) to that of the full-scale body. Since the projected frequency of maximum absorption for adult humans is on the order of 65–75 MHz in free space and about half as much in the presence of ground effects, the biological-phantom material that is used should have the dielectric properties of humans in that frequency range. A composition [9] of the material with 3.26 percent NaCl, 8.74 percent Superstuff (obtained from Whamo Manufacturing Company, San Gabriel, California), and 87.0 percent water has a measured dielectric constant of 66 and a conductivity of 4.39 mho/m. For use at a frequency of 350 MHz, this corresponds to $\epsilon_r = 66 - j225.6$. By comparison, for muscle, skin, and tissues with high water content, $\epsilon_r = 88 - j250$ at 50 MHz [4]. Because of the relative closeness of the two dielectric constants, the mixture of this composition was used to fill the figurine-shaped cavity for experiments in the parallel-plate radiation chamber.[7] Temperature under irradiation was recorded using the liquid-crystal temperature probe [8]. From the increase in temperature, the absorbed power density in milliwatts/gram was calculated from the relationship [7] (4180 × temperature increase)/irradiation time in seconds. The absorption coefficient $\alpha$,[8] defined as milliwatts/gram of absorbed power/milliwatts/square centimeter of incident field intensity for various parts of the body, has been calculated and is given in Table II. For $\boldsymbol{E} \parallel \hat{L}$ orientation, the strongest intensity of power deposition is observed in the neck area of the body. For the density of power absorption this is followed by the shins, the thighs, the chest, the eyes, and the pudendal region, in that order. In Fig. 7 the thermographic record of the temperature before and after 1 min of free-space irradiation with a field intensity of 100 mW/cm² at 710 MHz is shown. The pattern of power deposition bears a remarkable resemblance to the distribution obtained in the parallel-plate radiation chamber.

In order to obtain a quantitative information on the power deposition under free-space irradiation conditions, a 12.1-cm resonant-size ($L/\lambda \simeq 0.4$) figurine was used at 985 MHz.[9] A field intensity of 100 mW/cm² was used to

[6] The uniformity of fields in the central working area was established by heating a 19-cm-long saline-filled prolate spheroid in the $\boldsymbol{E} \parallel \hat{L}$ orientation. For the spheroid placed at the center of the plates, a temperature increase of 1.23°C was measured for an incident field intensity of 49.10 mW/cm² at 360 MHz. By comparison, a temperature increase of 1.15°C at 48.88 mW/cm² was observed for the same spheroid placed 10.2 cm off the center line.

[7] For free-space irradiation experiments, the composition of the material used is 9.25 percent NaCl, 8.25 percent Superstuff, and 82.5 percent water. This mixture, having a measured dielectric constant of 66 and a conductivity of 10.09 mho/m, corresponds to a complex relative permittivity $\epsilon_r$ of $66 - j255$ when used at 710 MHz.

[8] The parameters $S$ and $\alpha$ are related in that $S = (\alpha \times$ weight of the body)/(shadow area of the body). For animals and other bodies of irregular shape, $S$ is a more difficult parameter to calculate because of the difficulty in evaluating the shadow area of these bodies.

[9] E. L. Hunt of the Department of Microwave Research, Walter Reed Army Institute of Research, Washington, D. C., participated in these experiments.

TABLE II
MEASURED DISTRIBUTION OF POWER DEPOSITION IN AN 18.4-CM-TALL BIOLOGICAL-PHANTOM HUMAN FIGURINE (PARALLEL-PLATE WAVEGUIDE RADIATION CHAMBER)

| Frequency MHz | L/λ | α Neck | α Shin | α Eyes | α Pudendal Region |
|---|---|---|---|---|---|
| $\vec{E} \parallel \hat{L}$ orientation | | | | | |
| 230 | 0.141 | 2.895 | | | |
| 240 | 0.147 | 3.381 | 0.788 | | 0.155 |
| 270 | 0.166 | | 1.927 | | |
| 300 | 0.184 | 5.097 | 2.256 | 0.840 | 0.442 |
| 320 | 0.196 | 5.367 | | | |
| 350 | 0.215 | 6.761 | 1.863 | | |
| 380 | 0.233 | | 4.368 | 1.148 | |
| 395 | 0.242 | 6.153 | | | |
| $\vec{k} \parallel \hat{L}$ orientation | | | | | |
| 395 | 0.242 | 0.094 | | | |
| $\vec{H} \parallel \hat{L}$ orientation | | | | | |
| 300 | 0.184 | 0.130 | | | |

*Note:* Symbols with arrows above are represented by boldface italic in text.

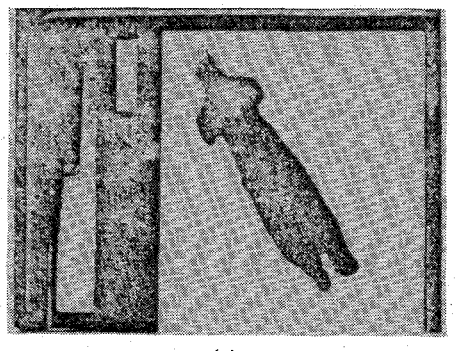

(a)

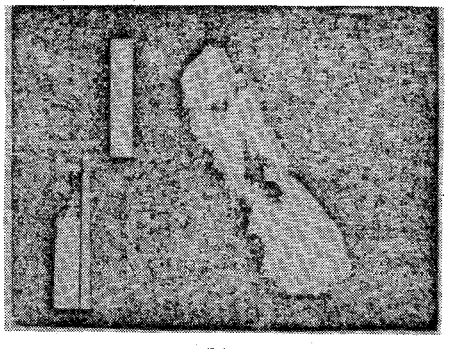

(b)

Fig. 7. The thermographic recording of the central section of an 18.4-cm biological-phantom figurine before and after free-space plane-wave irradiation for 1 min at 100 mW/cm² at 710 MHz ($L/\lambda \simeq 0.44$). (a) Before exposure to radiation, 8.5°C baseline; 3°C full scale. (b) After irradiation in the $\boldsymbol{E} \parallel \hat{L}$ configuration; waves incident on the front side of the body, 6°C baseline; 10°C full scale.

speed up the heating process and thus reduce the heat diffusion to cooler areas of the body. Temperature under irradiation was recorded using the liquid-crystal temperature probe. Due to the extremely large energy deposition rate for the neck region, exposure times on the order of 5 s were used when measuring temperature increases for this part of the body. Irradiation times of 10–20 s were used for measurements in other parts of the body. The measured rates of temperature rise are used to calculate the $\alpha$'s for various parts of the body in a 1.75-m man and these are given in Table III. The patterns of power deposition obtained from both the parallel-plate waveguide radiation chamber and free-space irradiation are very similar. For the $\boldsymbol{E} \parallel \hat{L}$ resonance condition, the very maximum power deposition is observed for the neck region of the body. Under both free-space and parallel-plate waveguide irradiation conditions, an $\alpha$ parameter of approximately 20 times the whole-body average is observed for the neck region of the body.

A point of concern is the much lower values observed in the parallel-plate radiation chamber as compared to the values measured under free-space irradiation. This may be seen by comparing the values in Table II to those of column 3 of Table III. The fact that a larger scaling factor $\beta$ is used for the 12.1-cm figurine than for the 18.4-cm figurine should account only for a factor of 1.52 in going from Table II to Table III. Somewhat reduced values in Table II will also be expected because of lower field intensities and the resultant heat diffusion, particularly from hot spots. In order to create a more satisfactory representation of the real-life ground effects, a monopole-above-ground radiation has been designed and is currently under construction at our laboratory. The new radiation chamber is sketched in Fig. 8. The radiator consists of a 45° corner reflector in conjunction with a quarter-wave monopole above ground. The gain of such an antenna has been calculated [10] and is tabulated in Table IV. For the antenna-to-corner spacing of 0.65 λ, the calculated radiation pattern of the antenna system is plotted in Fig. 9. The field intensity at a far-field distance of 6 ft for 350 W of radiated power may be as high as 60 mW/cm². Such field intensities are adequate for the planned experiments. The radiation chamber is being constructed with the provision for alterations for use at different frequencies in the 300–1000-MHz band. Such a radiation chamber is not easily amenable to wide-band whole-body absorption measurements such as have been possible in the parallel-plate transmission line using a network analyzer. The monopole-above-ground radiation chamber will, however, offer a real-life simulation of ground effects on EM power absorption in man and animals.

A significant result of the experiments with biological-phantom figurines is that a high power deposition in the neck region is observed. Power absorption coefficient $\alpha = 6.76$ for the neck region for $\boldsymbol{E} \parallel \hat{L}$ orientation is over 17 times larger than the average value for saline-filled prolate spheroids of the same overall dimension (see Table V for whole body or average $\alpha$ for a 19-cm saline-filled prolate spheroid at different frequencies). For $\boldsymbol{k} \parallel \hat{L}$ and $\boldsymbol{H} \parallel \hat{L}$ orientations, the rate of heating is minimal (Table II) and this, for the neck region, is a factor of 40 to 50 times smaller than the rate for the $\boldsymbol{E} \parallel L$ configuration. For these orientations the results once again are in agree-

TABLE III
RATES OF ENERGY DEPOSITION IN VARIOUS PARTS OF THE BODY
MEASURED DATA AND PROJECTED RATES OF ENERGY DEPOSITION IN A 1.75-M MAN

| Region of the Body | 985 MHz, Resonant Size (12.1 cm; L = 0.4 λ) Biological-Phantom Figurine | | 1.75 m Man, 67.9 MHz | | |
|---|---|---|---|---|---|
| | | | | Rate of Energy Deposition | |
| | Rate of Temperature Increase at 100 $mW/cm^2$ °C/Min. | α $(W/kgm)/(mW/cm^2)$ | α $(W/kgm)/(mW/cm^2)$ | For Incident Fields of 10 $mW/cm^2$ W/kgm | For Incident Fields of 50 $mW/cm^2$ W/kgm |
| Neck: | | | | | |
| Upper part | 128.3 | 89.38 | 6.16 | 61.62 | 308.10 |
| Lower part* | 65.2 | 45.42 | 3.13 | 31.31 | 156.57 |
| Shins | 9.5 | 6.62 | 0.46 | 4.56 | 22.80 |
| Thighs | 10.8 | 7.52 | 0.52 | 5.19 | 25.95 |
| Chest | 8.64 | 6.02 | 0.41 | 4.15 | 20.75 |
| Pudendal Region | 3.2 | 2.23 | 0.15 | 1.54 | 7.7 |
| Eyes | 0.9 | 0.63 | 0.043 | 0.43 | 2.15 |
| Arms | ? | ? | ? | ? | ? |

*Note:* $\boldsymbol{E} \parallel \hat{L}$ resonance condition ($L/\lambda = 0.4$).

* The rate of temperature rise for the lower part of the neck is considerably lower because of its vicinity close to the torso which provides a large heat drain.

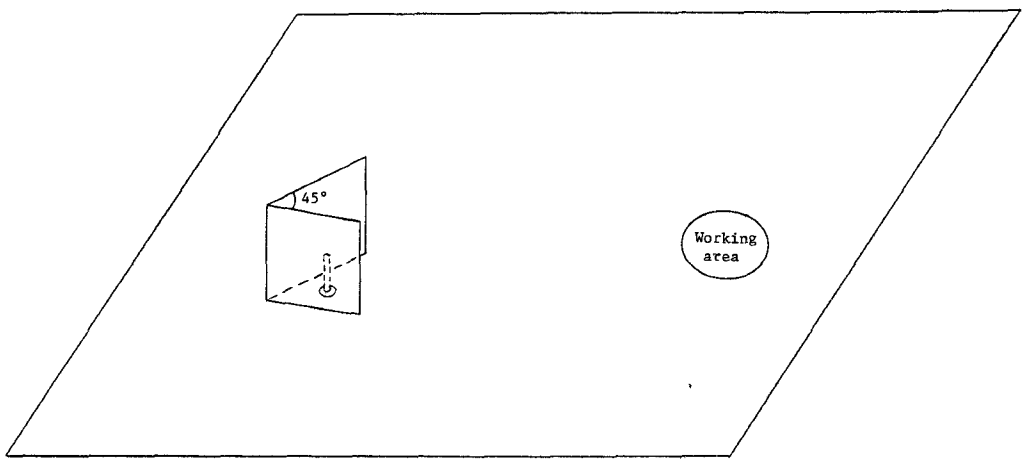


Fig. 8. A monopole antenna in a 45° corner reflector.

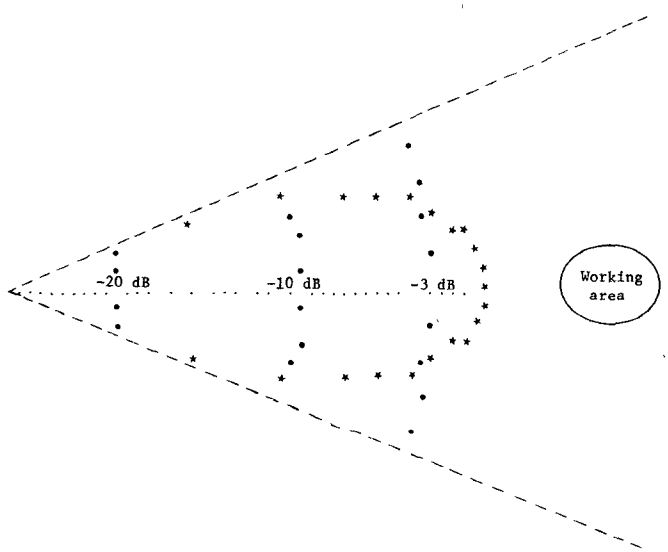


Fig. 9. Calculated radiation pattern at the ground plane of a monopole in a 45° corner reflector.

TABLE IV
CALCULATED FIELD INTENSITIES DUE TO A QUARTER-WAVE MONOPOLE IN A 45° CORNER REFLECTOR

| Distance to the Corner of the Reflector $\frac{S}{\lambda}$ | Driving Power Impedance Ohms | Calculated Gain of the Antenna | Field Intensity at R = 6 feet $mW/cm^2$ |
|---|---|---|---|
| 0.55 | 16 + j56.5 | 75 | 62.4 |
| 0.6 | 23.5 + j64.6 | 79.3 | 66.0 |
| 0.65 | 32 + j65.0 | 82.7 | 68.9 |
| 0.7 | 47.5 + j61.4 | 73.1 | 60.9 |
| 0.75 | 59.5 + j59.7 | 70.87 | 59.0 |

*Note:* Transmitter Power = 350 W.

TABLE V
ABSORPTION PARAMETER $\alpha$ OF A 19-CM SALINE-FILLED PROLATE SPHEROID AS A FUNCTION OF FREQUENCY

| Frequency MHz | Number of Measurements | $L/\lambda$ | $\alpha$ (average) |
|---|---|---|---|
| 240 | 1 | 0.152 | .2945 |
| 260 | 3 | 0.165 | .3097 |
| 300 | 3 | 0.190 | .2989 |
| 320 | 2 | 0.203 | .3214 |
| 360 | 3 | 0.229 | .4089 |
| 380 | 4 | 0.241 | .4908 |
| 395 | 4 | 0.251 | .3786 |

(a)

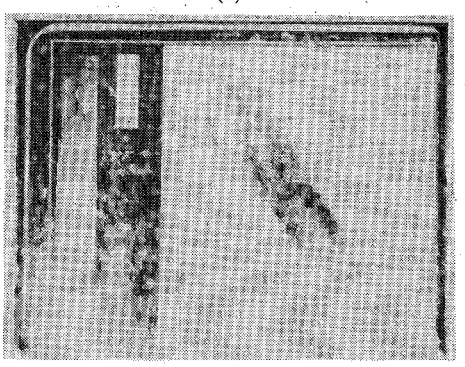

(b)

Fig. 10. Thermographic recording of the central section of an 18.4-cm biological-phantom figurine; free-space irradiation of 710 MHz (temperature of the body before irradiation $\simeq 7\frac{1}{8}$°C). (a) After irradiation in the $\boldsymbol{k} \parallel \hat{L}$ configuration for 10 min at 100 mW/cm²; baseline 8°C; 3°C full scale. (b) After irradiation in the $\boldsymbol{H} \parallel \hat{L}$ configuration for 10 min at 100 mW/cm²; baseline 8°C; 3°C full scale.

ment with those obtained from free-space irardiation. For up to 10 min of exposure to 710-MHz free-space fields of intensity 100 mW/cm², negligible modifications of the temperature pattern were observed, and this is illustrated in Fig. 10.

The thermographic record of the temperature before and after 1 min of free-space irradiation ($\boldsymbol{E} \parallel \hat{L}$ orientation) at 2450 MHz is shown in Fig. 11. Maximum heating at 2450 MHz ($L/\lambda = 1.5$), approximately 3.75 times the resonant frequency, is still observed in the neck, the arms, and the legs. As expected, the temperature rise is considerably lower than that for 710-MHz radiation. Also, the torso is heated hardly at all, which is a feature distinct from the power distribution at the resonant frequency of 710 MHz (Fig. 7). The quantitative values of $\alpha$ measured with

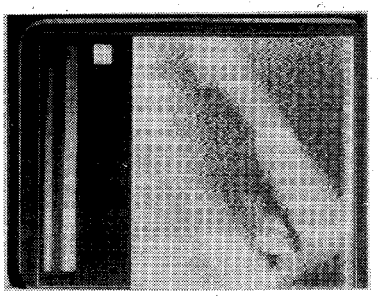

(a)

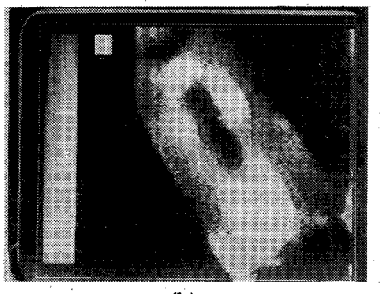

(b)

Fig. 11. The thermographic recordings of the central section of an 18.4-cm biological-phantom figurine before and after free-space plane-wave irradiation for 1 min at 100 mW/cm² at 2450 MHz ($L/\lambda = 1.50$). (a) Before exposure to radiation, 8.6°C baseline, 1°C full scale. (b) After irradiation in the $\boldsymbol{E} \parallel \hat{L}$ configuration; waves incident on the front side of the body; 10°C black level; 1°C full scale.

the liquid-crystal temperature probe for a somewhat smaller size figurine are given in Table VI. The hottest parts of the body are the neck, the legs, and the arms.

The large power deposition observed in the neck region of the figurines has prompted us to look for similar effects in animals. Initial measurements[10] conducted with the liquid-crystal probe implanted subcutaneously in the neck region of anesthetized 388-g long Evans rats have shown $\alpha = 0.479$ at 360 MHz as against $\alpha$ of 0.38 for the deep rectal region. For dead animals, on the other hand, the corresponding numbers are $\alpha = 0.855$ for the neck region and $\alpha = 0.231$ for the core of the animal. Further experiments are currently in progress to ascertain the nature of neck heating and its biological implications. Since reports in the literature suggest that continued low-level exposure to microwave irradiation in both humans [11] and animals [12] produces fatigue and hypoactivity, the possibility exists that this may be linked to the heating in the neck region. The heating in the neck area may produce changes in circulating blood hormones such as thyroxine. In future experiments, blood thyroxine levels will be examined by serum thyroxine and protein-bound iodine-level assay techniques.

## SUMMARY

The RF power deposition is found to vary significantly with orientation and with frequency. The strongest absorption is found for waves polarized along the long di-

[10] These experiments are being performed by J. D'Andrea of our laboratory.

TABLE VI
$E \parallel \hat{L}$, OFF-RESONANCE CONDITION ($L/\lambda = 0.985$)
MEASURED DATA AND PROJECTED RATES OF ENERGY DEPOSITION IN A 1.75-M MAN

| Region of the Body | 2450 MHz 12.1 cm Biological-Phantom Figurine $L/\lambda = 0.985$ | | 1.75 m Man, 169 MHz | | |
|---|---|---|---|---|---|
| | Rate of Temperature Increase at 100 $mW/cm^2$ °C/Min | $\alpha$ $(W/kgm)/(mW/cm^2)$ | $\alpha$ $(W/kgm)/(mW/cm^2)$ | Rate of Energy Deposition For Incident Fields of 10 $mW/cm^2$ W/kgm | Rate of Energy Deposition For Incident Fields of 50 $mW/cm^2$ W/kgm |
| Neck | 5.6 | 3.90 | 0.27 | 2.69 | 13.45 |
| Shins | 4.6 | 3.20 | 0.22 | 2.21 | 11.05 |
| Arms | 3.05 | 2.12 | 0.15 | 1.46 | 7.30 |
| Thighs | 2.05 | 1.43 | 0.1 | 0.99 | 4.95 |
| Chest | 1.2 | 0.84 | 0.06 | 0.58 | 2.9 |
| Eyes | 0.425 | 0.3 | 0.02 | 0.21 | 1.05 |
| Crotch | 0.2 | 0.14 | 0.01 | 0.1 | 0.5 |

mension of bodies at frequencies such that the major length is approximately 0.4 times the wavelength of radiation for bodies in free space. Peak absorption, in the presence of ground effects, is observed at frequencies about one-half as much as bodies isolated in free space. A significant result of the experiments with biological-phantom figurines is that a high rate of energy deposition is observed for the neck region. Power absorption coefficient $\alpha$ for the neck region for $\boldsymbol{E} \parallel \hat{L}$ orientation is about 20 times larger than the whole-body average. This may be biologically significant and is being investigated further. Initial experiments with anesthetized and dead rats have indeed demonstrated a higher power deposition in the neck region than in the core of the animals. For figurines for $\boldsymbol{k} \parallel \hat{L}$ and $\boldsymbol{H} \parallel \hat{L}$ orientations, the rate of heating is minimal, and for the neck region is a factor of 40 to 50 times smaller than the rate for the $\boldsymbol{E} \parallel \hat{L}$ resonance condition. The frequencies of maximum absorption for adult humans is projected to be on the order of 65–75 MHz for free-space conditions and about half as much in the presence of ground effects.

## ACKNOWLEDGMENT

The author wishes to thank E. L. Hunt who participated in parts of this work. The assistance of P. Brown and D. Hawkins of the Walter Reed Army Institute of Research is gratefully acknowledged. The author has also enjoyed the support of his students, in particular, J. D'Andrea, G. Beck, and T. Gustafson, in several facets of this work. The experiments with free-space irradiation were performed in the anechoic chambers at the Department of Microwave Research, Walter Reed Army Institute of Research, Washington, D. C.

## REFERENCES

[1] O. P. Gandhi, "Polarization and frequency effects on whole animal absorption of RF energy," *Proc. IEEE* (Lett.), vol. 62, pp. 1171–1175, Aug. 1974.
[2] ——, "Strongest dependence of whole animal absorption on polarization and frequency of radio-frequency energy," *Ann. N. Y. Acad. Sci.*, vol. 247, pp. 532–538, Feb. 1975.
[3] C. H. Durney, C. C. Johnson, and H. Massoudi, "Long-wavelength analysis of plane wave irradiation of a prolate spheroid model of man," *IEEE Trans. Microwave Theory Tech.*, vol. MTT-23, pp. 246–253, Feb. 1975.
[4] C. C. Johnson and A. W. Guy, "Nonionizing electromagnetic wave effects in biological materials and systems," *Proc. IEEE*, vol. 60, pp. 692–718, June 1972.
[5] T. B. A. Senior and R. F. Goodrich, "Scattering by a sphere," *Proc. Inst. Elec. Eng.*, vol. 111, pp. 907–916, 1964.
[6] J. Schrot, T. D. Hawkins, and S. H. Githens, "Microwave frequency and E-field orientation interact with animal size," presented at the 1975 USNC/URSI–IEEE Conf., Boulder, Colo., Oct. 20–23, 1975.
[7] A. Anne, M. Saito, O. M. Salati, and H. P. Schwan, "Relative microwave absorption cross sections of biological significance," in *Biological Effects of Microwave Radiation*, vol. 1. New York: Plenum, 1960, pp. 153–177.
[8] T. C. Rozzell, C. C. Johnson, C. H. Durney, J. L. Lords, and R. G. Olsen, "A nonperturbing temperature sensor for measurements in electromagnetic fields," *J. Microwave Power*, vol. 9, pp. 241–249, Sept. 1974.
[9] A. W. Guy, C. C. Johnson, J. C. Lin, A. F. Emery, and K. K. Kraning, "Electromagnetic power deposition in man exposed to HF fields and the associated thermal and physiologic consequences," USAF School of Aerospace Medicine, Brooks Air Force Base, Tex. Rep. SAM-TR-73-13, Dec. 1973
[10] O. P. Gandhi, "A computer program for calculating the radiation pattern of a general antenna array," *IEEE Trans. Educ.* (Corresp.), vol. E-17, pp. 124–126, May 1974.
[11] C. Silverman, "Nervous and behavioral effects of microwave radiation in humans," *J. Epidemiology*, vol. 97, pp. 219–224, Apr. 1973.
[12] S. F. Korbel, "Behavioral effects of low intensity UHF radiation," in *Proc. 1969 Symp. Biological Effects and Health Implications of Microwave Radiation*, Sept. 17–19, 1969.